ORIGINAL ARTICLE

Correlation between Quantified Breast Densities from Digital Mammography and 18F-FDG PET Uptake

Paras Lakhani, MD,* Andrew D. A. Maidment, PhD,* Susan P. Weinstein, MD,* Justin W. Kung, MD,† and Abass Alavi, MD*

*Department of Radiology, Hospital of the University of Pennsylvania, Philadelphia, Pennsylvania; and †Department of Radiology, Beth Israel Deaconess Medical Center, Boston, Massachusetts

Abstract: To correlate breast density quantified from digital mammograms with mean and maximum standardized uptake values (SUVs) from positron emission tomography (PET). This was a prospective study that included 56 women with a history of suspicion of breast cancer (mean age 49.2 ± 9.3 years), who underwent 18F-fluoro-2-deoxyglucose (FDG)-PET imaging of their breasts as well as digital mammography. A computer thresholding algorithm was applied to the contralateral nonmalignant breasts to quantitatively estimate the breast density on digital mammograms. The breasts were also classified into one of four Breast Imaging Reporting and Data System categories for density. Comparisons between SUV and breast density were made using linear regression and the Student's *t*-test. Linear regression of mean SUV versus average breast density showed a positive relationship with a Pearson's correlation coefficient of $R^2 = 0.83$. The quantified breast densities and mean SUVs were significantly greater for mammographically dense than nondense breasts ($p < 0.0001$ for both). The average quantified densities and mean SUVs of the breasts were significantly greater for premenopausal than postmenopausal patients ($p < 0.05$). 8/51 (16%) of the patients had maximum SUVs that equaled 1.6 or greater. There is a positive linear correlation between quantified breast density on digital mammography and FDG uptake on PET. Menopausal status affects the metabolic activity of normal breast tissue, resulting in higher SUVs in pre- versus postmenopausal patients. ■

Key Words: breast, digital, fluoro-2-deoxyglucose, mammography, positron emission tomography

Mammography is the only widely accepted modality for breast cancer screening (1–3), and has been shown to reduce breast cancer mortality (4–6). As such, the American College of Radiology and U.S. Preventive Services Task Force recommend that women 40 years or older should have routine screening mammograms (7,8). However, mammography is not a perfect screening tool and the sensitivity of mammography has been reported to be in the range of 75–90% with decreasing sensitivity with increasing breast density (1,3,4,9–14).

Fluoro-2-deoxyglucose positron emission tomography (FDG-PET) also has been evaluated for breast cancer detection (15–19). Similar to mammography, breast density may also affect FDG-PET interpretation. As denser breasts contain more fibroglandular tissue, the overall uptake of FDG is expected to be higher compared to nondense breasts, which potentially decreases the level of contrast between lesions and normal tissue on PET. In a prior retrospective study, Vranjesevic et al. (20) found that mammographically dense breasts had higher peak and mean standardized uptake values (SUVs) on FDG-PET than nondense breasts using a four-category Breast Imaging Reporting and Data System (BI-RADS) density grade estimate. Another analysis from Kumar et al. (21) also confirmed those results.

However, to our knowledge, no trial has been performed correlating mammographic breast density and FDG uptake on PET using a more quantifiable and objective measure of breast density. This may be particularly important as a quantifiable method for estimating breast density has been shown to be more precise than the BI-RADS classification (22). Furthermore, one should expect a more precise correlation when a semi-quantitative value such as SUV and quantifiable breast density are directly compared. In this study, we prospectively analyzed 56 women with a recent diagnosis or high suspicion of breast cancer who had PET imaging and bilateral digital mammograms.

Address correspondence and reprint requests to: Paras Lakhani, MD, Department of Radiology, Hospital of the University of Pennsylvania, 3400 Spruce Street, Philadelphia, PA 19104, USA, or e-mail: paras.lakhani2@uphs.upenn.edu.

DOI: 10.1111/j.1524-4741.2009.00737.x

We then correlated FDG uptake of their normal, cancer-free contralateral breasts with a semi-quantitative measure of breast density on digital mammography. Breast density was estimated using a computer-assisted thresholding algorithm [Cumulus 3 (University of Toronto, Ontario, Canada), courtesy of M. Yaffe, University of Toronto] that determines the percent composition of fibroglandular tissue on two-dimensional digital mammograms. Finally, we also evaluated the effects of menopausal status and age on mammographic breast density and FDG uptake.

MATERIALS AND METHODS

This study was approved by an institutional review board and was health insurance portability and accountability act compliant. All patients signed an informed consent prior to participation.

Study Design/Subjects

This was a secondary aim objective of a larger prospective National Institutes of Health (NIH) multimodality study for characterizing breast lesions and local-regional staging, funded for 400 women to receive bilateral breast magnetic resonance imaging (MRI), digital mammogram, film-screen mammogram, screening breast ultrasound, as well as a whole body ^{18}F-FDG PET scan. Women enrolled in this NIH study had with a recent diagnosis of breast cancer or a highly suspicious mammographic finding (BI-RADS; category 5).

This prospective study included 56 consecutive women (mean age 49.2 ± 9.3 years) enrolled in the above NIH study who had a digital mammogram and whole body ^{18}F-FDG PET scan obtained during the same day between 2003 and 2005. Patients were excluded from this particular study if they had bilateral breast cancer, a history of recent breast biopsy of a nonmalignant breast lesion, a history of having received chemotherapy and/or radiation therapy, or a suspicion of malignancy in the contralateral breast based on any of the imaging findings. The menopausal status was recorded for all but one enrolled patient.

FDG-PET Imaging

Patients underwent FDG-PET imaging of their breasts using a standard whole body PET scanner

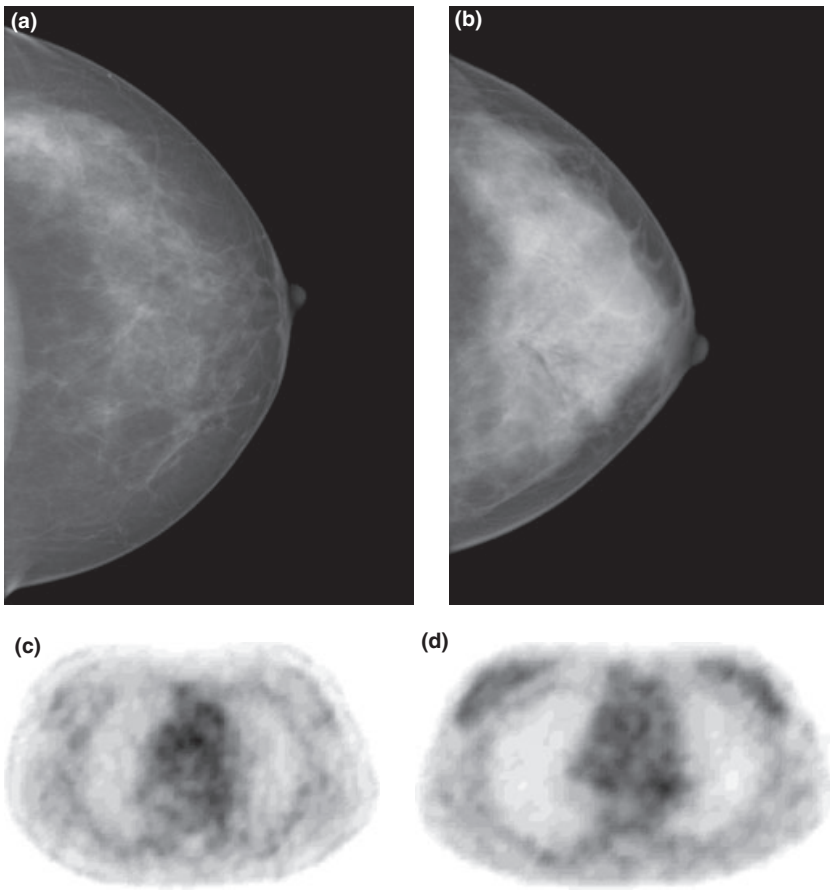

Figure 1. Comparison of mammographic density and FDG uptake in corresponding patients. (a) Cranial-caudal digital mammogram of a nondense breast (BI-RADS; category 2) with a quantified breast density of 20.16%. (b) Cranial-caudal digital mammogram of a dense breast (BI-RADS; category 3) with a quantified breast density of 52.85%. (c) FDG-PET image of nondense breasts corresponding to the same patient in (a) (Avg SUV = 0.27). (d) FDG-PET image of dense breasts corresponding to the same patient in (b) (Avg SUV = 0.51).

(Allegro; Philips Medical Systems, Philadelphia, PA). All participants fasted for at least 6 hours prior to injection of 5.2 MBq (0.14 mCi)/kg of ^{18}F-FDG, and had a confirmed serum glucose level below 140 mg/dL measured from a venous source. PET imaging was performed 60 minutes after injection, and patients were imaged in the supine position. Sequential overlapping emission scans of the neck, chest, abdomen, and pelvis were acquired. Postinjection transmission scans were obtained, according to previously published methods (23), using a ^{137}Cs point source. Images were reconstructed using an iterative reconstruction algorithm, and attenuation-corrected images were interpreted.

Standardized uptake values of the entire breast were calculated using the following formula: SUV = radioactivity in regions of interest (ROI) (Bq/mL)/injected dose (Bq)/body weight (g). ROI were drawn around the contralateral nonmalignant breasts in every transaxial slice containing breast tissue by a researcher in our division (PL), and was verified by a nuclear medicine physician (>20 years of experience with PET imaging). The average SUV for the entire breast was calculated using a weighted average that factored the area of the breast per ROI and the average SUV per ROI in each slice.

Digital Mammography

All patients underwent digital mammography using a Senographe 2000D system (General Electric Medical Systems, Milwaukee, WI). Routine cranio-caudal (CC) and mediolateral-oblique (MLO) views were obtained. A computer-assisted thresholding algorithm was used to quantitatively estimate the breast densities of the contralateral, cancer-free breasts in both the MLO and CC projections (24). This value was expressed as a percentage of dense pixels over the total number of pixels comprising the entire breast. This was performed by drawing a ROI encompassing the dense areas of the breast, which was facilitated by the Cumulus software [Cumulus 3, courtesy of M. Yaffe, University of Toronto] (Fig. 2). The ROIs were drawn by a researcher in our department (PL). This was done 2 months after the PET images were interpreted to reduce the effects of recall bias. In addition, mammographers from our breast imaging division (4–20 years of experience), independently categorized the breasts in a blinded fashion into one of four categories using the BI-RADS density criteria—entirely fatty (1), scattered fibroglandular densities (2), heterogeneously dense (3), or extremely dense (4).

Statistical Analysis

Linear regression analysis was performed between mean SUV and average quantified breast density for the contralateral breasts, and Pearson's correlation coefficients were calculated. Pearson's correlations were also calculated comparing quantified breast density to maximum SUV and patient age. In addition, the two-tailed, unpaired Student's *t*-test was used to determine whether differences existed between the patient subgroups, including pre- and postmenopausal patients, and those with clinically dense (BI-RADS; category 3, 4) and nondense breasts (BI-RADS; category 1, 2). $p < 0.05$ was considered statistically significant.

RESULTS

Five of the 56 women were excluded from this study because they did not meet the entry criteria. Three patients were excluded because they had a history of prior biopsies of the contralateral breasts. One patient was excluded due to an abnormal MRI finding that was suggestive of malignancy. The last patient

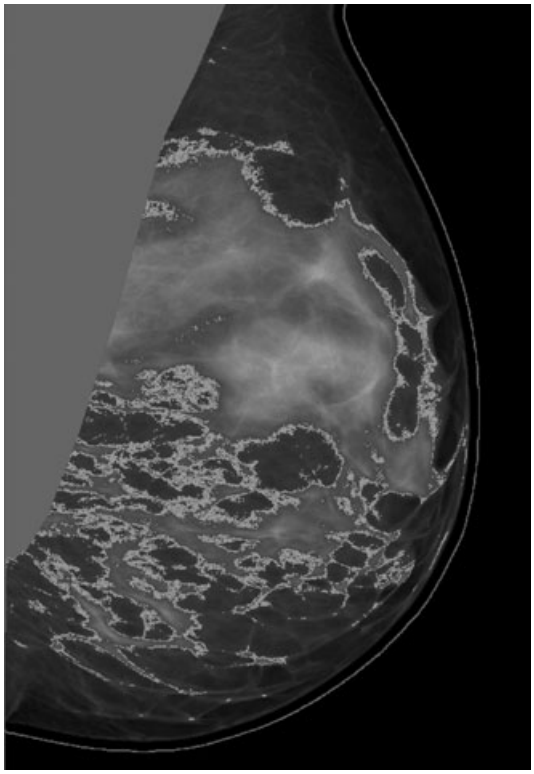

Figure 2. Digital mammogram in the MLO view. A region of interest is drawn around the glandular breast tissue depicted within a gray margin, facilitated by the Cumulus software. The pectoralis muscle is removed from the density measurement. There is a line outlining the skin.

was excluded due to a focal area of high FDG uptake on the PET scan that was suspicious for malignancy.

Of the 51 women who did meet entry criteria, the average SUVs of the normal contralateral breasts ranged from 0.23 to 0.63 (mean: 0.40 ± 0.11), and maximum SUVs ranged from 0.60 to 1.90 (mean: 1.22 ± 0.28). On digital mammography, the breast densities ranged from 8.71% to 69.75% on the MLO orientation (mean: 35.33% ± 16.86%), 8.48% to 69.31% on the CC orientation (mean: 36.49% ± 17.13%), and 8.60% to 66.93% using the average of the MLO and CC values (mean: 35.91% ± 16.74%).

For the nondense breasts (BI-RADS; category 1, 2), the average SUV was 0.32 ± 0.04, maximum SUV was 1.12 ± 0.29, and average quantified density was 21.06% ± 6.77%. For the dense breasts (BI-RADS; category 3, 4), the average SUV was 0.46 ± 0.10, maximum SUV was 1.29 ± 0.26, and average quantified density was 46.30% ± 13.43% (Table 1).

A linear regression plot of the mean SUV versus quantified breast density had a Pearson's correlation coefficient of $R^2 = 0.82$ in the MLO view, 0.79 in the CC view, and 0.83 using the average quantified density from these two views (Fig. 3a). A linear regression plot of the maximum SUV versus breast density showed a Pearson's correlation coefficient of $R^2 = 0.15$ in the MLO view, $R^2 = 0.14$ in the CC view, and $R^2 = 0.15$ using the average quantified density from these two views (Fig. 3b).

With the two-tailed, unpaired Student's *t*-test, the mean and maximum SUVs were significantly higher for dense (BI-RADS; category 3, 4) than nondense breasts (BI-RADS; category 1, 2) using the BI-RADS density criteria ($p < 0.0001$ for mean SUV, $p < 0.03$ for maximum SUV) (Table 1). The average breast density of the CC and MLO views were also significantly higher for dense versus nondense breasts ($p < 0.0001$) (Table 1).

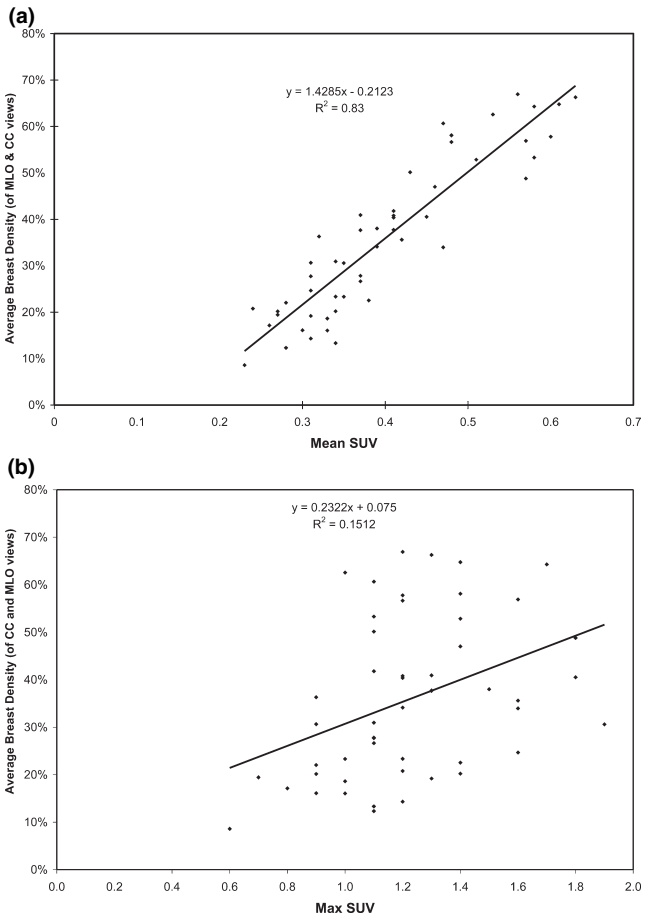

Figure 3. Scatter plots of average quantified density versus mean SUV (a) and maximum SUV (b). Linear regression analysis show a Pearson's correlation of $R^2 = 0.83$ and $R^2 = 0.15$ for average density versus mean and maximum SUV, respectively.

Menopausal status was known for 50 of the 51 women in the study. Of the 50 patients, 26 were premenopausal, 19 were postmenopausal, and five were peri-menopausal. None of the patients including

Table 1. Standardized Uptake Values and Quantified Average Breast Densities by Group

Group	*n*	Mean SUV	Maximum SUV	MLO density	CC density	Average density (CC and MLO)
All patients	51	0.40 ± 0.11	1.22 ± 0.28	35.3% ± 16.9%	36.5% ± 17.1%	35.9% ± 16.7%
Nondense (BI-RADS 1,2)	21	0.32 ± 0.04	1.12 ± 0.29	21.5% ± 7.5%	20.7% ± 7.0%	21.1% ± 6.8%
Dense (BI-RADS 3,4)	30	0.46% ± 0.10	1.29 ± 0.26	45.0% ± 14.6%	47.5% ± 12.8%	46.3% ± 13.4%
Significance		p < 0.0001	p < 0.03	p < 0.0001	p < 0.0001	p < 0.0001
Premenopausal*†	26	0.43 ± 0.11	1.30 ± 0.24	39.3% ± 15.9%	41.0% ± 15.0%	40.1% ± 15.0%
Postmenopausal*†	19	0.37 ± 0.10	1.14 ± 0.30	32.0% ± 18.1%	32.5% ± 19.2%	32.2% ± 18.6%
Significance		p < 0.05	p < 0.05	p < 0.17	p < 0.10	p < 0.12

*None of the patients were on hormone replacement therapy.
†Five of the 51 patients were perimenopausal, and menopausal status was not known in one patient.
SUV, standardized uptake values; MLO, mediolateral-oblique; CC, cranio-caudal; BI-RADS, Breast Imaging Reporting and Data System.

postmenopausal patients were taking hormone replacement therapy or birth control. For the premenopausal patients, the average SUV ranged from 0.27 to 0.63 (mean: 0.43 ± 0.11), the maximum SUV ranged from 0.90 to 1.90 (mean: 1.30 ± 0.24), and the average density of the CC and MLO views ranged from 12.33% to 66.93% (mean: 40.09% ± 15.03%). For the postmenopausal patients, the average SUV ranged from 0.23 to 0.58 (mean: 0.37 ± 0.10), the maximum SUV ranged from 0.60 to 1.80 (mean: 1.14 ± 0.30), and the average density of the CC and MLO views ranged from 8.60% to 64.29% (mean: 32.22% ± 18.55%) (Table 1). Using the Student's *t*-test, the mean and maximum SUVs were significantly higher for pre- versus postmenopausal patients ($p < 0.05$ for mean SUV, and $p < 0.05$ for maximum SUV) (Table 1). The average density was found to be higher for the pre- versus postmenopausal patients, but this was not statistically significant ($p < 0.12$).

To examine the effect of age on breast density, a linear regression plot of patient age versus average quantified breast density of the MLO and CC values showed a Pearson's correlation coefficient of $R^2 = 0.03$ (Fig. 4a). A linear regression plot of patient age versus mean SUV showed a Pearson's correlation coefficient of $R^2 = 0.06$ (Fig. 4b). To determine the significance of the above regression coefficients, two-tailed *t*-tests for the regression coefficients were performed. It was determined that the trend of age versus average breast density and mean SUV were not statistically significant, and appeared as independent variables.

A segmental analysis of the normal contralateral breasts, transaxially divided into 10 equal parts from superior to inferior, showed that the majority of the FDG uptake occurred in the central areas of the breasts for both mean and maximum SUVs (Fig. 5). Representative images showing the visual differences between dense and nondense breasts on PET and digital mammography are presented in Figure 1.

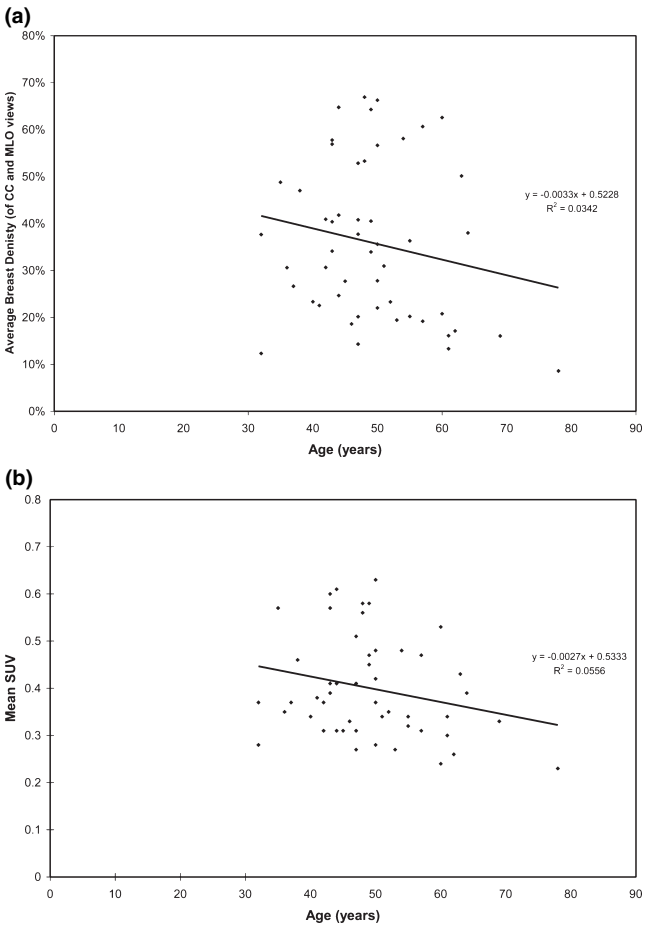

Figure 4. Scatter plots of average quantified density (a) and mean SUV (b) versus age. Linear regression analysis show a Pearson's correlation of $R^2 = 0.03$ and $R^2 = 0.06$ for average density and mean SUV versus age, respectively.

DISCUSSION

To our knowledge, this is the first study comparing SUV with a semi-quantitative estimate for mammographic breast density. In this study, we used a computer thresholding algorithm on digital mammograms, in addition to the BI-RADS density criteria, to provide a more objective and quantifiable estimate of breast density. In so doing, we were able to more precisely correlate these values with SUVs on PET.

The computer-thresholding algorithm [Cumulus 3] is a two-dimensional interactive program that estimates the percent of nonadipose tissue that comprises the breast on MLO and CC projections using digital mammograms, which is expressed as a percentage (Fig. 2). The software sets a density threshold that approximates the difference between fibroglandular and fatty tissue, which is derived from calibration experiments from tissue equivalent plastic phantoms (24). This program estimates breast density using two projections and thus true volumetric breast density measurements are not possible. In our study population, the mean breast density for the MLO position was 35.55% ± 16.86%, and 36.49% ± 17.13% for the CC position, showing good concordance in the density values between the two views.

We correlated the quantified density values from digital mammograms with both average and maximum SUVs from FDG-PET. The average SUVs

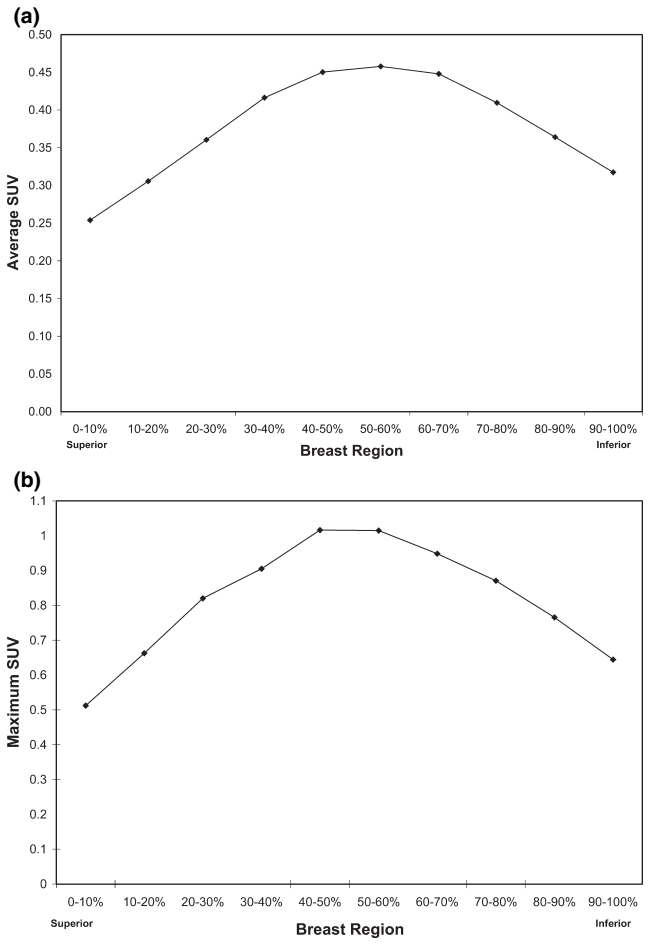

Figure 5. Plots of mean (a) and maximum (b) SUV per breast region. In these graphs, the breast regions are divided into 10 equal segments from superior to inferior for all of the patients in the study. For each of the segments, an average of the mean and maximum SUVs are determined, and plotted versus their corresponding breast region. The highest FDG activity corresponds to the central breast.

showed a strong positive correlation with quantified density from digital mammography, with a Pearson's correlation coefficient of $R^2 = 0.82$ in the MLO view, 0.79 in the CC view, and 0.83 using the average density from these two views (Fig. 3a). The average SUV was determined using a weighted average of the entire breast, factoring the area and mean SUV per transaxial slice. Thus, the average SUVs correlated well with the average quantified breast density values, which represented the percent composition of fibroglandular tissue in the MLO and CC projections. As fibroglandular tissue is more metabolically active than fatty tissue, one would expect to see an overall higher uptake of FDG in denser breasts. On the other hand, we found a weak correlation with maximum SUV on PET and breast density, showing a Pearson's correlation coefficient of $R^2 = 0.15$ in the MLO view, 0.14 in the CC view, and 0.15 using the average density from these two views (Fig. 3b). As maximum SUV represents the highest foci of FDG uptake in the breast, rather than the average metabolic activity of the entire breast, we did not expect a positive correlation between maximum SUV and average quantified breast density.

We also found that both average SUV and breast density were significantly greater in dense than nondense breasts categorized by the BI-RADs density grade estimate ($p < 0.0001$) (Table 1). As average SUV correlates well with average quantified breast density, as shown by the high Pearson's correlation coefficient of 0.83, one would expect to find that both average SUV and average breast density would show similar statistically significant results. While maximum SUV showed a weak correlation with breast density, as mentioned above, we found a significant difference in maximum SUVs between dense and nondense breasts ($p < 0.03$) categorized by BI-RADs breast density (Table 1).

We performed a linear regression of patient age versus average quantified breast density and average SUV on PET, and found a Pearson's correlation coefficient of $R^2 = 0.03$ and $R^2 = 0.06$ respectively (Fig. 4). While it has been shown that average mammographic breast density declines with age (25–27), we did not find this true for our patient population. However, the number of patients in those studies was considerably larger, and we feel that our sample size was not large enough to detect such trends.

On the other hand, although the breast density did not statistically decrease with age in our patients, we found that average and maximum SUVs were significantly higher in pre- versus postmenopausal patients ($p < 0.05$) (Table 1). Reports in the literature have also shown that hormonal status may correlate better with mammographic density than age (28–32). Similar statistically significant results were shown by Vranjesevic et al. (20), but not Kumar et al. (21). While quantifiable breast density was higher in pre- versus postmeopausal patients, this was not significantly different ($p < 0.12$). This may indicate that older women with dense breasts tend to have a greater amount low metabolic fibrous tissue, while younger women with dense breasts have a proportionately greater amount of more metabolically active glandular tissue. It should be noted that none of the patients were on

birth control or hormone replacement therapy at the time of the study.

For the normal contralateral breasts in this study, the average maximum SUV was 1.22 ± 0.28, and the highest maximum SUV found was 1.9. This is higher than that found by Vranjesevic et al., who reported a highest maximum SUV of 1.39. It is known that SUV measurements may vary based on many factors, including the timing of scanning following FDG injection, manufacturer of the scanner, lean body mass of the patient, and ROI measurements (31,32). In addition, our patient population differed in that we measured the normal contralateral breasts in patients with a recent diagnosis of breast cancer or high suspicious mammographic finding. It is plausible that one or a number of the above factors may have contributed to differences in reported maximum SUVs. However, the timing of our PET scanning following FDG injection was nearly identical to that Vranjesvic et al. (20). Moreover, it has been shown that lean body mass correction has little effect on the SUV for lower metabolic regions such as normal breast tissue (20,32). Thus, the other factors may have had an impact on the differences in our reported values, or it is plausible that the background measurements for dense breasts are higher than previously reported.

The average SUVs for mammographically dense and nondense breasts were very similar to that reported by Vranjesevic et al. (20), but lower than that of Kumar et al. (21). However, a different methodology was used in the latter study, in which representative measurements of breast tissue were analyzed rather than the entire breast. For example, we noticed that if the inferior and superior margins of the breast are included, which predominately contain fatty tissue (Fig. 5), the average SUVs are substantially reduced. As we used the same methodology as Vranjesevic et al., our results were similar.

In eight of the 51 patients (16%), the normal contralateral breasts had maximum SUVs of 1.6 or greater. Seven of these eight patients (88%) had mammographically dense breasts. Seventy-five percent of those patients were premenopausal (five patients) or perimenopausal (one patient), and 25% were postmenopausal (two patients). Therefore, it is plausible that sensitivity for primary breast cancer detection with FDG-PET may be reduced in patients with high breast background FDG activity, including premenopausal patients and those with mammographically dense breasts. This may be more applicable for low metabolic tumors such as well differentiated or lobular carcinoma (18,19,33,34) which have been shown to demonstrate low tumor-to-background uptake. However, further research with a dedicated study is warranted to demonstrate this. This may also help explain the high variability in the reported sensitivity of FDG-PET for primary breast carcinoma, ranging from 63% to 96% (35–37).

We also noticed that the pattern of FDG uptake was higher towards the center of the breast relative to the absolute periphery. Thus, the average and maximum SUVs were higher in the central areas of the breast, where there is a combination of adipose and fibroglandular tissue, rather than the absolute periphery, where there is predominately adipose tissue in the layer of subcutaneous fat (38). While it is known that glandular tissue is typically most concentrated in the upper outer quadrant of the breast (39), the patient is imaged on PET while supine, which causes the inferior aspects of the breast to shifted more superiorly. Thus, the distribution of FDG uptake on axial slices correlates well with the expected geometry of the breast during PET imaging and the expected distribution of glandular tissue.

There are limitations to this study. The computer thresholding algorithm [Cumulus] provides a two-dimensional estimate of mammographic density. While this is more precise than the subjective BI-RADS breast density classification, this does not provide a measure of volumetric breast density. In future studies, it would be interesting to compare volumetric breast density or MRI with FDG-PET uptake values. In addition, this was a secondary aim paper from a larger multimodality study characterizing breast lesions and local-regional staging. The study was performed analyzing the normal nonmalignant breasts of patients with a history or suspicion of contralateral breast cancer. Perhaps different results would be found in patients with bilateral mammographically normal breasts. It should be noted, however, that all of the normal breasts were determined to be free of malignancy from digital mammography, MRI imaging of the breast and PET.

CONCLUSIONS

There is a positive linear correlation between quantified breast density from digital mammography and mean SUV on FDG-PET. Mammographically dense breasts have higher mean and maximum SUVs than

nondense breasts. Menopausal status affects the metabolic activity of normal breast tissue, resulting in higher SUVs in pre- versus postmenopausal patients. The pattern of FDG uptake tends to correlate with the expected distribution of glandular tissue in the breast. Eight of the 51 patients (16%) had maximum SUVs of 1.6 or greater, mostly consisting of premenopausal patients and those with mammographically dense breasts. Further research is warranted to demonstrate if the sensitivity for FDG-PET in primary breast carcinoma is consequently affected in such patients.

Acknowledgments

This research was funded in part by the National Institutes of Health grant 1 PO1 CA085484, and a Fellowship Award from the Society of Nuclear Medicine. The authors wish to acknowledge Dr. Martin J. Yaffe, University of Toronto, for providing the Cumulus 3 software, and for technical discussions.

REFERENCES

1. Rosenberg RD, Hunt WC, Williamson MR, *et al.* Effects of age, breast density, ethnicity, and estrogen replacement therapy on screening mammographic sensitivity and cancer stage at diagnosis: review of 183,134 screening mammograms in Albuquerque, New Mexico. *Radiology* 1988;209:511–8.

2. Baines CJ, Miller AB, Wall C, *et al.* Sensitivity and specificity of first screen mammography in the Canadian National Breast Screening Study: a preliminary report from five centers. *Radiology* 1986;160:295–8.

3. Humphrey LL, Helfand M, Chan NK, *et al.* Breast cancer screening: a summary of the evidence for the U.S. Preventive Services Task Force. *Ann Intern Med* 2002;137:347–60.

4. Fletcher SW, Black W, Harris R, *et al.* Report of the International Workshop on Screening for Breast Cancer. *J Natl Cancer Inst* 1993;85:1644–56.

5. Tabar L, Fagerberg G, Chen HH, *et al.* Efficacy of breast cancer screening by age. New results from the Swedish Two-County Trial. *Cancer* 1995;75:2507–17.

6. Frisell J, Klund G, Hellstrom L. Randomized study of mammography screening: preliminary report on mortality in the Stockholm trial. *Breast Cancer Res Treat* 1991;18:49–56.

7. Weir HK, Thun MJ, Hankey BF, *et al.* Annual report to the nation on the status of cancer, 1975–2000, featuring the uses of surveillance data for cancer prevention and control. *J Natl Cancer Inst* 2003;95:1276–99.

8. Feig SA, D'Orsi CJ, Hendrick RE, *et al.* American College of Radiology guidelines for breast cancer screening. *AJR Am J Roentgenol* 1998;171:29–33.

9. Kerlikowske K, Grady D, Barclay J, *et al.* Effect of age, breast density, and family history on the sensitivity of first screening mammography. *JAMA* 1996;276:33–8.

10. Kolb TM, Lichy J, Newhouse JH. Comparison of the performance of screening mammography, physical examination, and breast US and evaluation of factors that influence them: an analysis of 27,825 patient evaluations. *Radiology* 2002;225:165–75.

11. Mushlin AI, Kouides RW, Shapiro DE. Estimating the accuracy of screening mammography: a meta-analysis. *Am J Prev Med* 1998;14:143–53.

12. Salvatore M, Del Vecchio S. Dynamic imaging: scintimammography. *Eur J Radiol* 1998;27:S259–64.

13. Mandelson MT, Oestreicher N, Porter PL, *et al.* Breast density as a predictor of mammographic detection: comparison of interval- and screen-detected cancers. *J Natl Cancer Inst* 2000;92:1081–7.

14. Lehman CD, White E, Peacock S, *et al.* Effect of age and breast density on screening mammograms with false-positive findings. *AJR Am J Roentgenol* 1999;173:1651–5.

15. Nieweg OE, Kim EE, Wong WH. Positron emission tomography with fluorine-18-deoxyglucose in the detection and staging of breast cancer. *Cancer* 1993;71:3920–5.

16. Hoh CK, Schiepers C. 18-FDG imaging in breast cancer. *Semin Nucl Med* 1999;29:49–56.

17. Adler LP, Crowe JP, al-Kaisi NK, Sunshine JL. Evaluation of breast masses and axillary lymph nodes with [F-18] 2-deoxy-2-fluoro-D-glucose PET. *Radiology* 1993;187:743–50.

18. Buck A, Schirrmeister H, Kuhn T, *et al.* FDG uptake in breast cancer: correlation with biological and clinical prognostic parameters. *Eur J Nucl Med Mol Imaging* 2002;29:1317–23.

19. Avril N, Dose J, Janicke F, *et al.* Metabolic characterization of breast tumors with positron emission tomography using F-18 fluorodeoxyglucose. *J Clin Oncol* 1996;14:1848–57.

20. Vranjesevic D, Schiepers C, Silverman DH, *et al.* Relationship between 18F-FDG uptake and breast density in women with normal breast tissue. *J Nucl Med* 2003;44:1238–42.

21. Kumar R, Chauhan A, Zhuang H, *et al.* Standardized uptake values of normal breast tissue with 2-deoxy-2-[F-18]fluoro-D: -glucose positron emission tomography: variations with age, breast density, and menopausal status. *Mol Imaging Biol* 2006;8:355–62.

22. Martin KE, Helvie MA, Zhou C, *et al.* Mammographic density measured with quantitative computer-aided method: comparison with radiologists' estimates and BI-RADS categories. *Radiology* 2006;240:656–65.

23. Smith R, Karp J, Muehllehner G, *et al.* Singles transmission scans performed post-injection for quantitative whole body PET imaging. *IEEE Trans Nucl Sci* 1997;44:1329–35.

24. Byng JY, Boyd NF, Fishell E, *et al.* Automated analysis of mammographic densities. *Phys Med Biol* 1996;41:909–23.

25. Stomper PC, D'Souza DJ, DiNitto PA, *et al.* Analysis of parenchymal density on mammograms in 1353 women 25–79 years old. *AJR Am J Roentgenol* 1996;167:1261–5.

26. Wolfe JN. Breast parenchymal patterns and their changes with age. *Radiology* 1976;121:545–52.

27. Oza AM, Boyd NF. Mammographic parenchymal patterns: a marker of breast cancer risk. *Epidemiol Rev* 1993;15:196–208.

28. Laya MB, Larson EB, Taplin SH, *et al.* Effect of estrogen replacement therapy on the specificity and sensitivity of screening mammography. *J Natl Cancer Inst* 1996;88:643–9.

29. Thurfjell EL, Holmberg LH, Persson IR. Screening mammography: sensitivity and specificity in relation to hormone replacement therapy. *Radiology* 1997;203:339–41.

30. Grove JS, Goodman MJ, Gilbert FI Jr, Mi MP. Factors associated with mammographic pattern. *Br J Radiol* 1985;58:21–5.

31. Huang SC. Anatomy of SUV. Standardized uptake value. *Nucl Med Biol* 2000;27:643–6.

32. Zasadny KR, Wahl RL. Standardized uptake values of normal tissues at PET with 2-[fluorine-18]-fluoro-2-deoxy-D-glucose: variations with body weight and a method for correction. *Radiology* 1993;189:847–50.

33. Crippa F, Seregni E, Agresti R, *et al.* Association between [18F]fluorodeoxyglucose uptake and postoperative histopathology, hormone receptor status, thymidine labelling index and p53 in primary breast cancer: a preliminary observation. *Eur J Nucl Med* 1998;25:1429–34.

34. Avril N, Menzel M, Dose J, *et al.* Glucose metabolism of breast cancer assessed by 18F-FDG PET: histologic and immunohistochemical tissue analysis. *J Nucl Med* 2001;42:9–16.

35. Schirrmeister H, Kuhn T, Guhlmann A, *et al.* Fluorine-18 2-deoxy-2-fluoro-d-glucose PET in the preoperative staging of breast cancer: comparison with the standard staging procedures. *Eur J Nucl Med Mol Imaging* 2001;28:351–8.

36. Rose C, Dose J, Avril N. Positron emission tomography for the diagnosis of breast cancer. *Nucl Med Commun* 2002;23:613–8.

37. Walter C, Scheidhauer K, Scharl A, *et al.* Clinical and diagnostic value of preoperative MR mammography and FDG-PET in suspicious breast lesions. *Eur Radiol* 2003;13:1651–6.

38. Gray H. The mammae. In: Gray H, Lewis WH, eds. *Anatomy of the Human Body*. Philadelphia, PA: Lea & Febiger, 1918; Bartleby.com, 2000:1267–8.

39. Feig SA, Orel SG, Dershaw DD. The breast. In: Grainger RB, Allison D, Adam A, Dixon A, eds. *Grainger & Allison's Diagnostic Radiology: a Textbook of Medical Imaging*. New York, NY: Churchill Livingstone, 2001:2239–75.